

Analysis of the Thermal and Magnetic Properties of Amorphous Ribbons of $\text{Fe}_{61}\text{Co}_{10}\text{B}_{20}\text{Y}_8\text{Me}_1$ (where $\text{Me} = \text{W}, \text{Zr}, \text{Nb}, \text{Mo}$)

P. PIETRUSIEWICZ* AND M. NABIAŁEK

Institute of Physics, Faculty of Production Engineering and Materials Technology,
Częstochowa University of Technology, al. Armii Krajowej 19, 42-200 Częstochowa, Poland

This paper presents the results pertaining to thermal and magnetic studies of rapidly-cooled samples of the alloy family $\text{Fe}_{61}\text{Co}_{10}\text{B}_{20}\text{Y}_8\text{Me}_1$ (where $\text{Me} = \text{Nb}, \text{Zr}, \text{W}, \text{Mo}$). The resulting ribbons, or tapes, have amorphous structure. It has been found that the addition of Me elements alters the thermal and magnetic properties. It is noted that the saturation magnetization decreases with increasing number of unpaired electrons on the valence shells. In addition, the value of the coercivity and effective anisotropy have been determined.

DOI: [10.12693/APhysPolA.131.678](https://doi.org/10.12693/APhysPolA.131.678)

PACS/topics: 61.43.Dq, 75.50.Kj, 65.60.+a, 75.30.Gw

1. Introduction

Amorphous alloys that feature so-called soft magnetic properties have been known for over 50 years [1, 2]. The interest in these alloys continues unabated, due to their unique properties and manifold opportunities to create new alloy compositions. One of the most interesting aspects of amorphous materials is the difficulty in describing them on the basis of their structure. The reason for this is the irregular structure of these alloys, since, in a thermodynamic sense, they are in a metastable state with higher values of free energy than crystalline materials (which are thermodynamically stable). Therefore, the commonly used description of crystalline materials, based on Bernal groups, does not apply to amorphous materials. It is interesting to note that, until the 1970s, the domain structure existing within amorphous material inevitably was linked with crystalline materials. The strength of this belief was such that, even when amorphous material had been obtained (as indicated by structural studies), it was claimed that it was a crystalline material because it exhibited magnetic properties.

Recent studies have revealed that significantly better soft magnetic properties are obtained in materials featuring amorphous structure, compared with alloys having the same chemical composition but featuring crystalline structure [2–5]. This development has substantially increased the interest in these materials; in turn, this has resulted in the development of apparatus for their preparation. Concurrently, many methods have been developed, which have enabled the production of amorphous alloys. Initially, the end-products of most methods were samples with nanometric thickness, which rendered them very difficult to use in practice. However, during this pe-

riod, one of the most powerful and well-known production methods was developed: the method featuring unidirectional cooling of molten alloy on a rotating cylinder (i.e. melt spinning). Using this method, it is possible to obtain a solid sample in the form of a ribbon, with a thickness of several μm to several dozens μm [6, 7]. Achievements made using this method have substantially widened the range of potential applications for this class of materials. This production technique was quickly introduced to industry [8].

The interest in amorphous materials increased rapidly, and, to this day, has shown no sign of declining. Currently, the application is widespread [2, 8]. When manufactured in the form of a soft magnetic ribbon or tape, the resulting product has found applications in electrical engineering and electronics [2, 8]. Transformer cores made from such materials are energy efficient and environmentally friendly, in comparison with the commonly-used FeSi transformer laminations. However, the main advantages of magnetic cores made from amorphous materials are their excellent magnetic properties: low core loss, low value of coercive field, relatively high saturation magnetization (depending on the alloy, 0.7–1.7 T) and almost zero magnetostriction [9]. It has been found that changes in the magnetic properties of amorphous alloys are very sensitive to slight changes in the chemical composition: changes of the order of a few percent. Due to the metastable nature of these alloys, the thermal stability is also an important parameter.

This paper presents the results obtained for the rapidly-cooled alloy family $\text{Fe}_{61}\text{Co}_{10}\text{B}_{20}\text{Y}_8\text{Me}_1$ in the form of ribbons, where $\text{Me} = \text{Nb}, \text{Zr}, \text{W}, \text{Mo}$. Gaining an understanding of the impact of small changes in the chemical composition of amorphous alloys is a fundamental requirement for determining their structure and enabling a fuller description of their microstructure. This information is critical when it comes to classifying and matching properties and applications.

*corresponding author; e-mail: pietrusiewicz@wip.pcz.pl

2. Experimental procedure

The investigated samples were prepared using the following component elements, all featuring atomic purity of > 99.98%: Fe, Co, Y, Zr, W, Nb, and Mo; the element boron was added in the form of FeB alloy. Homogenised ingots were cast in an electric arc furnace, ready for the next stage: the preparation of the tape samples. The ingot samples were divided into smaller portions, which were then used for the rapid cooling process on the rotating copper cylinder. Both the crystalline ingots and tapes were prepared under an inert atmosphere.

X-ray diffraction profiles were taken for the investigated tapes using a Bruker D8 Advance X-ray diffractometer. The X-ray diffractometer operated in the Bragg-Brentano geometry ($\text{Cu } K_\alpha$). The measurement was performed over a 2θ -angle range of 30° to 100° with a measuring step-size of 0.2° and exposure time of 5 s. Measurements of differential scanning calorimetry (DSC) were performed using NETZSCH equipment. The samples were heated under an Ar atmosphere, from room temperature up to the liquidus temperature of ≈ 1500 K, at a constant heating rate of 10 K/min. Static magnetic hysteresis loops and curves of the primary magnetization were measured in a magnetic field intensity of up to 2 T using a LakeShore vibrating sample magnetometer.

3. Results of the investigations

X-ray diffraction patterns for the samples of the investigated alloys in ribbon form are shown in Fig. 1.

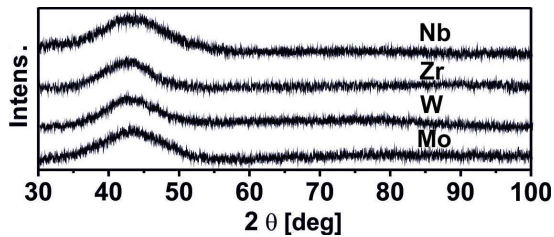


Fig. 1. X-ray diffraction patterns for the ribbon-form samples of the investigated alloy family: $\text{Fe}_{61}\text{Co}_{10}\text{B}_{20}\text{Y}_8\text{Me}_1$, where $\text{Me} = \text{Nb}, \text{Zr}, \text{W}, \text{Mo}$.

The X-ray diffraction patterns, presented in Fig. 1, are typical for amorphous materials; they feature only one, broad, maximum in the 2θ -range of 35° – 55° . Above this range, only the low intensity background could be observed.

The thermal stability of the alloys was analysed on the basis of the DSC measurements (Fig. 2).

The curves obtained from the analysis of heat flow as a function of temperature are similar for all of the alloys. The crystallisation process for all of the samples consists of two stages: primary and secondary. From the DSC curves, the glass transition temperatures (T_g) have been determined. The extent of the supercooled liquid range, the glass transition temperature and the crystallisation onset temperature (T_x) for each of the investigated alloys have been presented in Table I. Despite the fact that the

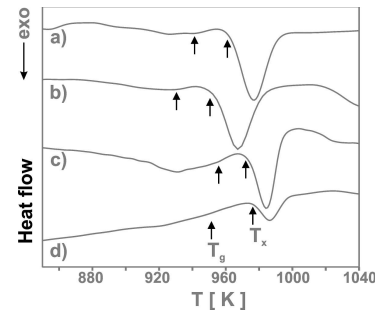


Fig. 2. DSC curves obtained for the ribbon-form samples of the investigated alloy family: $\text{Fe}_{61}\text{Co}_{10}\text{B}_{20}\text{Y}_8\text{Me}_1$, where $\text{Me} = \text{Nb}$ (a), Zr (b), W (c), and Mo (d).

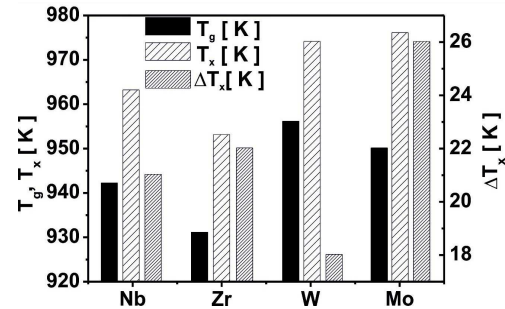


Fig. 3. Diagram of T_x , T_g and ΔT_x vs. addition of $\text{Me} = \text{Nb}, \text{Zr}, \text{W}, \text{Mo}$, for $\text{Fe}_{61}\text{Co}_{10}\text{B}_{20}\text{Y}_8\text{Me}_1$.

extent of the supercooled liquid range ΔT_x is relatively small, all of the investigated samples possess amorphous structure. The dependence between temperatures T_g and T_x , and the temperature range ΔT_x , resulting from the addition of Me , have been presented in Fig. 3.

The alloy with the addition of Mo — the element which destabilises the magnetic structure the most — showed the lowest crystallisation onset temperature. Mo is also an element which causes decrease of the Curie temperature and the saturation magnetisation. Key parameters, obtained from analysis of the static hysteresis loops and initial magnetisation curves are assembled in Table I.

TABLE I

Data from analysis of the static hysteresis loops (VSM) for $\text{Fe}_{61}\text{Co}_{10}\text{B}_{20}\text{Y}_8\text{Me}_1$, $\mu_0 M_S$ — saturation magnetization, H_k — anisotropy field, H_c — coercivity, K_{eff} — effective anisotropy.

	$\mu_0 M_S$	H_c	H_k	K_{eff}	T_g	T_x	ΔT_x
Me	[T]	[A/m]	[kA/m]	[kJ/m ³]	[K]	[K]	[K]
Nb	1.38(2)	101(5)	61(5)	46(6)	942	963	21
Zr	1.33(2)	35(3)	49(5)	37(6)	931	953	22
W	1.49(2)	61(3)	102(5)	78(6)	956	974	18
Mo	1.31(2)	186(5)	68(5)	44(6)	950	976	26

As can be seen from the data presented in Table I, the best soft magnetic properties have been found for the alloy containing W, which, as shown in [10], in small quantities (up to 2 at.%) was found to stabilise magnetic

structure. The surprise is to find the highest value of the effective anisotropy for the alloy with the addition of 1 at.% of W. This state could be connected with the preservation of the magnetisation in the higher magnetic fields. This could be explained by the large quantity of structural defects, which could delay an increase in the value of the magnetisation while approaching the region above the field of the effective anisotropy. Figure 4 shows the relationships of M_S and H_c with the addition of Me: Nb, Zr, W, Mo, all for the $\text{Fe}_{61}\text{Co}_{10}\text{B}_{20}\text{Y}_8\text{Me}_1$ alloy.

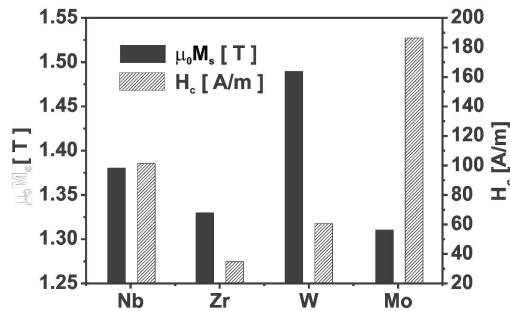


Fig. 4. Relationship of M_S and H_c versus the addition of Me = Nb, Zr, W, Mo for $\text{Fe}_{61}\text{Co}_{10}\text{B}_{20}\text{Y}_8\text{Me}_1$.

In the case of the addition of either Nb or Zr, each of these elements influences the glass-forming ability of the amorphous materials in a different way. Nb is being added as a nanocrystallisation catalyst, whereas Zr is being added as a component stabilising the amorphous state during the production process. In the case of small additions of Zr or Nb, their standard behaviour is different from the description presented above. Element Nb does not generate nanocrystalline structure (and as a result an increase in the saturation magnetisation and decrease in the coercivity). This behaviour regarding H_c could be rather observed in the case of the addition of Zr, which in small quantities causes an increase in the value of the stiffness parameter of the spin wave D_{spf} [7].

4. Conclusions

The melt-spinning technique allowed for the production of amorphous samples of the alloy family: $\text{Fe}_{61}\text{Co}_{10}\text{B}_{20}\text{Y}_8\text{Me}_1$ (where Me = W, Zr, Nb, Mo). The addition of Me in the quantity of 1 at.% was found to influence strongly the magnetic properties of the investigated alloys, preserving their amorphous structure. In the case of the investigated alloys, their magnetic structure depends strongly on the addition of Me. It has been shown that the value of the saturation magnetisation of the studied alloys depends strongly on the basic properties of the components used as the Me additions. The main contributors to the magnetic properties are the free electrons, which are not taking part in the bonding process between atoms, and regions featuring fluctuations in their composition and density. This also means that the distribution of the Me addition within the investigated alloys is not homogeneous; this influences the re-configuration of the atoms within the volume of the alloy. These reconfigurations occur at various energy levels,

which could explain the two-stage crystallisation process in the investigated alloys: primary and secondary. The glass transition temperatures and the extent of the supercooled liquid range have been determined. The extent of the supercooled liquid region has been found to be less than 20 K.

In general, for the investigated alloys, the extent of this region is small, which could suggest poor glass-forming ability. As has been shown in [6, 7, 11], for the investigated alloy compositions, it is possible to obtain bulk amorphous alloys — despite the narrow value of ΔT_x observed for these alloys. This is quite important because it stresses that, in the process of designing the chemical composition for bulk amorphous alloys, the results of investigations performed on samples in the form of ribbons should not be decisive as they are made with totally different parameters. These minor changes in alloy composition have a relatively major influence on the values of the saturation magnetisation and the coercivity. While the changes in the magnetisation are relatively easy to explain [6, 7, 11], the sudden increase in the coercivity for the samples where Me=Nb and Mo, is quite complicated. The regions with varying density hinder the free movement of the domain walls and therefore the increase in the coercive field must be taken into account. Within these regions, or on their boundaries, “transitions” between atoms occur; or to be more specific, the structural re-orientation of the atomic axis within the “free volumes”. In these cases, these regions should be treated as some kind of “crystalline grains” in the amorphous matrix, causing pinning of the domain walls and an increase in the value of the coercivity [12].

References

- [1] P. Duwez, S.C.H. Lin, *J. Appl. Phys.* **38**, 4096 (1967).
- [2] M.E. McHenry, M.A. Willard, D.E. Laughlin, *Prog. Mater. Sci.* **44**, 291 (1999).
- [3] H.S. Chen, *Rep. Progr. Phys.* **43**, 353 (1980).
- [4] A. Inoue, in: *Bulk Amorphous Alloys*, Eds. A. Inoue, K. Hashimoto, Springer-Verlag, Berlin 2001.
- [5] A. Inoue, A. Takeuchi, *Acta Mater.* **59**, 2243 (2011).
- [6] M. Nabiałek, P. Pietrusiewicz, K. Błoch, *J. Alloy Comp.* **628**, 424 (2015).
- [7] P. Pietrusiewicz, M. Nabiałek, M. Szota, M. Dośpiał, K. Błoch, A. Bukowska, K. Gruszka, *Arch. Metall. Mater.* **59**, 659 (2014).
- [8] *Metglas company history*.
- [9] G. Herzer, *Acta Mater.* **61**, 718 (2013).
- [10] M. Nabiałek, M. Dośpiał, M. Szota, P. Pietrusiewicz, J. Jędryka, *J. Alloy Comp.* **509**, 3382 (2011).
- [11] P. Pietrusiewicz, M. Nabiałek, M. Dośpiał, K. Gruszka, K. Błoch, J. Gondro, P. Brągiel, M. Szota, Z. Stradomski, *J. Alloy Comp.* **615**, S67 (2014).
- [12] H. Kronmüller, *J. Magn. Magn. Mater.* **24**, 159 (1981).